4. M. Kondo *et al.*, *ibid.* **262**, 1874 (1993); M. Noguchi *et al.*, *ibid.*, p. 1877; S. M. Russell *et al.*, *ibid.*, p. 1880.
5. C. J. McMahan *et al.*, *EMBO J.* **10**, 2821 (1991).
6. S. Gillis and K. A. Smith, *Nature* **268**, 154 (1977).
7. B. J. Brandhuber, T. Boone, W. C. Kenney, D. B. McKay, *Science* **238**, 1707 (1987); J. F. Bazan, *ibid.* **257**, 410 (1992).
8. J. F. Bazan, *Immunol. Today* **11**, 350 (1990).
9. S. Srinivasan, C. J. March, S. Sudarsanam, *Protein Sci.* **2**, 277 (1993).
10. K. Grabstein and M. Kennedy, personal communication.
11. J. Yodoi *et al.*, *J. Immunol.* **134**, 1623 (1985).
12. T. Takeshita *et al.*, *J. Exp. Med.* **169**, 1323 (1989).
13. J. Suzuki *et al.*, *Int. Immunol.* **1**, 373 (1989).
14. J. S. Greenberger *et al.*, *Fed. Proc.* **42**, 2762 (1983).
15. PBTs were selected from fresh PBMCs by E-rosette formation, and $CD4^+$ and $CD8^+$ subsets were further isolated by antibody affinity to paramagnetic microspheres with magnetic cell sorter (MACS, Miltenyi Biotec, Sunnyvale, CA). T cells were activated for 72 hours with PHA followed by 24 hours in IL-2–containing medium. T cell blasts were then harvested, washed, and used. Test cultures contained 50,000 T cells per culture or 2000 CTLL cells per culture. Culture medium was supplemented as described [K. Grabstein *et al.*, *J. Exp. Med.* **163**, 1405 (1986)], and 0.5 μCi of [^{3}H]thymidine was added for the last 4 hours of culture. Cells were collected onto glass fiber filters and radioactivity was determined by avalanche gas ionization.
16. PBMCs, prepared from fresh whole blood by Ficoll Hypaque density gradient centrifugation, were activated by culture with PHA as described above for PBTs (*15*).
17. IL-15 was purified from 64 liters of supernatant of CV-1/EBNA cells by ultrafiltration (YM-30), hydrophobic chromatography (Phenyl Sepharose CL-4B), anion-exchange chromatography (DEAE Sephacel and Mono Q fast protein liquid chromatography), reversed-phase HPLC (C4, 5 μm) eluted with an acetonitrile gradient in 0.1% trifluoroacetic acid (TFA) [D. L. Urdal *et al.*, *J. Chromatogr.* **296**, 171 (1984)], reversed-phase HPLC eluted with an n-propanol gradient in TFA, and SDS-PAGE.
18. Proteins were electroblotted from the SDS gel to a PVDF membrane. The protein band corresponding to the IL-15 activity was cut out, and the sequence of the 33 NH_2-terminal residues was determined by Edman degradation. Two degenerate oligonucleotide mixtures encoding all possible codon usages of residues 1 to 6 and the complement of all possible codon usages of residues 26 to 31 (omitting position 3 of Val^{31}) were synthesized. First-strand cDNA synthesized from CV-1/EBNA mRNA was amplified by PCR with the oligonucleotide mixtures as primers. This yielded a 92-bp DNA fragment that was cloned into pBluescript SK^-. A hybridization probe prepared from this DNA fragment was used to isolate a cDNA clone containing the complete IL-15 coding region from a cDNA library constructed from CV-1/EBNA mRNA essentially as described [D. M. Anderson *et al.*, *Cell* **63**, 235 (1990)].
19. A simian IL-15 probe was prepared by labeling of the purified simian IL-15 cDNA with random primers. Northern blot analysis with this probe identified the human IMTLH bone marrow–derived stromal cell line as a source of human IL-15 mRNA. Southern (DNA) blots of pools of an IMTLH cDNA library were probed to identify a positive pool and subsequently to isolate a human IL-15 cDNA.
20. A PCR-generated DNA fragment, containing the simian IL-15 coding region minus the 48–amino acid leader sequence, was ligated into a yeast expression vector that directs secretion of the recombinant protein into the yeast medium [V. Price *et al.*, *Gene* **55**, 287 (1987)]. Recombinant IL-15 was purified from the yeast supernatant as described above for the CV-1–derived IL-15 protein, excluding ultrafiltration and ion exchange. The purity and concentration of IL-15 were confirmed by amino acid analysis.
21. Human PBMCs from one donor (5×10^5 per culture) were cultured with irradiated PBMCs (5×10^5 per culture) from either an allogeneic donor (CTL) or from the autologous donor (LAK) in cultures containing various concentrations of either IL-2 or IL-15, or no cytokine. Cultures were done as described [M. B. Widmer *et al.*, *J. Exp. Med.* **166**, 1447 (1987)] and harvested after 6 days (LAK) or 7 days (CTL) and assayed for cytolytic activity against ^{51}Cr-labeled targets. The lysis assay contained various numbers of the responding peripheral blood lymphocytes cultured with 1000 labeled targets in 200 μl of medium in V-bottomed wells, and supernatants were collected after 4 hours of incubation. Lytic units were calculated as the inverse of the fraction of the responding culture required to generate 50% (CTL) or 30% (LAK) of the maximum specific ^{51}Cr release.
22. Mikβ1 was purchased from Nichirei Corp., Tokyo, Japan; TU11 and TU27 were provided by K. Sugamura, Sendai, Japan; 2A3 was produced at Immunex.
23. C. W. Dunnett, *J. Am. Stat. Assoc.* **50**, 1096 (1955).
24. Activated PBMCs (*16*) were incubated for 2 hours in medium without PHA or growth factors. IL-15 and IL-2 binding were carried out at 4°C for 60 min in RPMI 1640 containing 3% bovine serum albumin and 0.1% $NaNO_3$. IL-2 and IL-15 were radiolabeled as described [L. Park *et al.*, *J. Biol. Chem.* **261**, 4177 (1986)] and retained biological activity. Preliminary experiments established that equilibrium binding was obtained under these conditions (J. Giri and M. Ahdieh, personal communication).
25. YT cells used are a subclone of the human NK-like YT cell line and were provided by M. Caligiuri, Roswell Park Memorial Institute, Buffalo, NY.
26. We thank S. D. Lupton and R. J. Tushinski for the IMTLH cDNA library, T. Hollingsworth for DNA sequence analysis, C. J. March and M. Gerhart for protein sequence analysis, R. Jerzy for the cDNA cloning plasmid, J. King for the yeast expression construct, T. W. Tough and L. Erickson for technical assistance, and M. B. Widmer and M. K. Spriggs for reviewing the manuscript.

22 November 1993; accepted 4 April 1994

Enhancer Point Mutation Results in a Homeotic Transformation in *Drosophila*

Mary Jane Shimell, Jeffrey Simon, Welcome Bender, Michael B. O'Connor*

In *Drosophila*, the misexpression or altered activity of genes from the bithorax complex results in homeotic transformations. One of these genes, *abd-A*, normally specifies the identity of the second through fourth abdominal segments (A2 to A4). In the dominant *Hyperabdominal* mutations (*Hab*), portions of the third thoracic segment (T3) are transformed toward A2 as the result of ectopic *abd-A* expression. Sequence analysis and deoxyribonuclease I footprinting demonstrate that the misexpression of *abd-A* in two independent *Hab* mutations results from the same single base change in a binding site for the gap gene *Krüppel* protein. These results establish that the spatial limits of the homeotic genes are directly regulated by gap gene products.

The establishment of correct segmental identity in *Drosophila melanogaster* requires the proper function and expression of genes located in the antennapedia and bithorax complexes [reviewed in (*1–3*)]. In the bithorax complex, loss-of-function mutations typically result in transformations of posterior segments toward more anterior fates, whereas the ectopic activation of homeotic genes along the anterior-posterior axis produces dominant, gain-of-function phenotypes in which anterior segments are transformed toward more posterior identities (*4–8*). The initial activation of homeotic gene expression appears to be regulated by the segmentation gene products (*9–15*). For example, mutations in the gap gene *hunchback* (*hb*) result in an anterior shift of *Ubx* expression (*12*), whereas mutations in *Krüppel*, *knirps*, and *giant* cause ectopic activation of *Abd-B* (*13–16*). In several cases, incomplete homeotic regulatory elements containing *hb* binding sites have been shown to confer spatially restricted patterns of gene expression when positioned next to a *LacZ* reporter gene (*9–11*). However, as a result of the large size of homeotic regulatory regions (50 to 100 kb), the precise roles of these individual elements within the context of a complete regulatory domain has remained elusive.

We have studied the *Hab-1* and *Hab-2* mutations, two gain-of-function alleles that ectopically express the *abd-A* protein (ABD-A). The *Hab-1* and *Hab-2* alleles were discovered by E. B. Lewis and I. Duncan, respectively, and Lewis has proposed that they likely affect a homeotic regulatory element (*4*, *15*). The *Hab* mutations cause dominant transformations of portions of T3 toward A2 as a result of

M. J. Shimell and M. B. O'Connor, Department of Molecular Biology and Biochemistry and Developmental Biology Center, University of California, Irvine, CA 92717, USA.
J. Simon, Department of Biochemistry, University of Minnesota, St. Paul, MN 55108, and Department of Biological Chemistry and Molecular Pharmacology, Harvard Medical School, Boston, MA 02115, USA.
W. Bender, Department of Biological Chemistry and Molecular Pharmacology, Harvard Medical School, Boston, MA 02115, USA.

*To whom correspondence should be addressed.

ectopic *abd-A* expression (*4*, *6*, *17*). The most common phenotype observed is the loss of haltere or third leg (or both) (*4*, *17*). Less frequently, a transformation of haltere toward wing is also observed (*18*). When originally isolated, the *Hab-1* allele occasionally caused a partial transformation of A1 toward A2 (*4*). In recent analysis, this transformation is not observed. We attribute the difference to the accumulation of genetic modifiers in the stock, because the penetrance and expressivity of the phenotype can be enhanced in certain genetic backgrounds (*17*). We have also found that the penetrance of the phenotype is dependent on temperature. Approximately 9% of individuals who inherit the *Hab-2* chromosome show some type of transformation at 18°C, 35% show transformation at 25°C, and 50% show a phenotype at 29°C. An examination of *abd-A* expression in *Hab* mutant embryos reveals that *abd-A* protein is expressed anterior to its normal parasegment 7 (PS 7) boundary within PS 5 and a portion of PS 6 (Fig. 1, A and B) (*6*). This pattern of misexpression is consistent with the observed transformations.

Recombination experiments have placed *Hab-1* within the *abd-A* gene and associated regulatory sequences (*4*, *17*). This region encompasses approximately 80 kb of DNA that includes the 30-kb *abd-A* transcription unit as well as 50 kb of 5′ regulatory sequences. In previous reports, mutations that ectopically activate homeotic genes have been shown to be associated with chromosomal aberrations (*19*–*23*). These lesions have included insertions, deletions, and translocations that rearrange regulatory sequences in the non-coding portions of these genes. In contrast, Southern blot analysis of *Hab* mutations failed to detect any aberrations along the entire length of the *abd-A* transcription unit and within the 50 kb of upstream regulatory DNA (*24*).

If the *Hab* alleles are point mutations, we reasoned that they must affect one of the regulatory elements that direct *abd-A* expression. We have described an 11-kb fragment from the large *abd-A* intron (Fig. 2A) that directs the expression of a *LacZ* reporter construct with an anterior boundary in PS 7 (*25*). The sequences responsible for directing this pattern in early embryos were narrowed to a 1.7-kb Sal I–Xba I fragment by a series of hybrid dysgenesis-induced deletions of the 11-kb fragment and by an additional *LacZ* germline transformation construct (Fig. 2A). We have referred to the regulatory sequences that control the early boundaries of homeotic expression patterns as initiator elements (*25*, *26*) and refer to this particular fragment as the *iab-2(1.7)* initiator.

To test whether the *Hab-1* mutation was located within the minimal *iab-2(1.7)* initiator sequence, transformant lines were made with the *Hab-1* 1.7-kb *Sal I–Xba I* fragment inserted upstream of a *LacZ* reporter gene (*27*). Transformant embryos containing *Hab-1* sequences driving *LacZ* show an early ectopic stripe of *LacZ* expression in PS 5 at the cellular blastoderm stage as well as a band of staining within the central block that is wider and more intense than that of transformant embryos containing wild-type (WT) *iab-2(1.7)* sequences (Fig. 1, C and D). The ectopic expression persists during gastrulation, and, by the completion of germ-band extension, the pattern of *LacZ* misexpression is similar to that of ABD-A misexpression (Fig. 1, B and F). These results demonstrate that the lesion associated with the *Hab-1* phenotype is located within the *iab-2(1.7)* fragment.

The *Hab-1* lesion was identified by the sequencing of the 1.7-kb *Hab-1* fragment and the equivalent fragment from a stock containing the background chromosome on which *Hab-1* was induced (*28*). A single G to A transition was identified at base 251 within the *Hab-1* fragment (Fig. 2B). To determine whether the *Hab-2* chromosome also contained a lesion at or near this site, a 285–base pair (bp) fragment centered about the *Hab-1* mutation (Fig. 2B) was amplified from *Hab-2* hemizygous DNA by polymerase chain reaction (PCR) and sequenced (*28*). The same G to A transition was identified in the *Hab-2* DNA. There were four DNA sequence polymorphisms found on the *Hab-2* chromosome and its parent but not on *Hab-1* and its background chromosome (Fig. 2B). These polymorphisms demonstrate that these two lesions are the result of independent mutational events.

To reveal which regulatory proteins

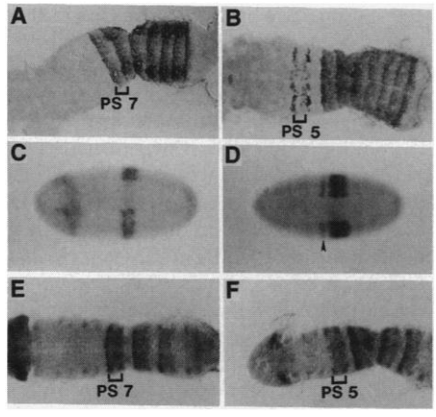

Fig. 1. ABD-A misexpression caused by a mutation in the *iab2(1.7)* fragment. (**A**) A dissected (*6*), wild-type (WT) embryo at the germband extended stage (6 hours of development) stained with ABD-A antibody. The PS 7 anterior limit of ABD-A expression is indicated with a bracket. For all embryos, anterior is on the left. (**B**) A dissected *Hab-2* embryo showing misexpression of ABD-A in PS 5 and PS 6. (**C** and **E**) Expression of *LacZ* directed by the *iab-2(1.7)* fragment and (**D** and **F**) the equivalent fragment from an *Hab-1* chromosome. (C) and (D) are ventral views of early gastrulation embryos, whereas (E) and (F) show dissected germband extended embryos. Embryos in (C) and (D) were hybridized to antisense, digoxigenin-labeled *LacZ* RNA (*27*), whereas embryos in (E) and (F) were stained with a *LacZ* antibody (*27*). Note the anterior ectopic stripes of *LacZ* activity directed by the *Hab* fragment [bracket in (B) and arrowhead in (D)]. The location of the WT band of *LacZ* staining in (C) has been positioned by the double-staining of embryos with digoxigenin-labeled *LacZ* RNA probes and antibodies to *ftz* and *eve*. For (E), we previously determined that the location of the anterior staining boundary directed by the *iab-2* enhancer is located at the PS 6–PS 7 border (*25*).

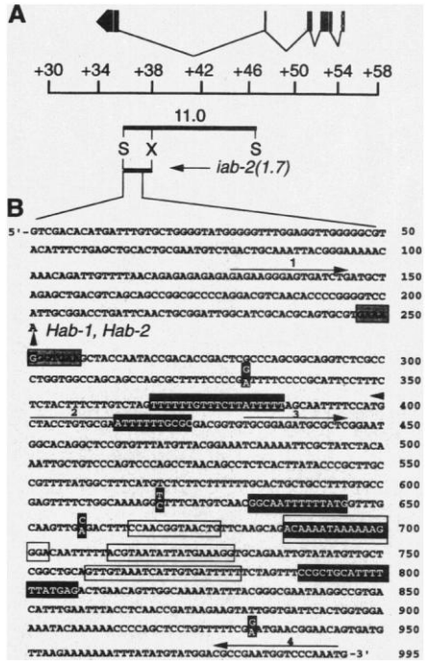

Fig. 2. Location of the *Hab-1* and *Hab-2* mutations. (**A**) Physical map of the *abd-A* transcription unit and the locations of the *iab-2(11)* and *iab-2(1.7)* fragments within the large intron. Diagnostic restriction sites are Sal I (S) and Xba I (X). (**B**) Sequence of that portion of the *iab-2(1.7)* fragment that binds gap and pair-rule gene products (*28*, *31*). The location of the *Hab* mutations are indicated with an arrow. The four single-base polymorphisms that distinguish *Hab-1* from the *Hab-2* chromosome are highlighted in reverse type. The lower base is found in the Canton S and *Hab-2* chromosomes, while the upper base is found in the bx^8 and *Hab-1* chromosomes (*28*). The KR binding site disrupted by the *Hab* mutations is enclosed in the stipled box. Additional sites protected by EVE are outlined by the clear box, while HB sites are enclosed in the black boxes (*31*).

might control the *iab-2* initiator element, we introduced the WT *iab-2(1.7) LacZ* expression construct into various gap and pair-rule mutant backgrounds (*29*). In a *Krüppel* mutant, we observed ectopic stripes of lacZ expression in PS 5 similar to that exhibited in *Hab-1* mutants. An examination of the sequence surrounding the *Hab* base change revealed that the altered G base was imbedded in the sequence GAAAGGGTGAA, which matches a consensus *Kr* protein (KR) binding site in 9 out of 11 bases (*30*). Gel shift and deoxyribonuclease (DNase) I footprinting experiments were conducted to determine whether KR bound to this site or other sites in the *iab-2(1.7)* sequence. A gel mobility-shift analysis of *iab-2(1.7)* sequences revealed that KR binds to only a single fragment that contains the consensus KR binding site (*31*). The DNase I footprinting of *iab-2(1.7)* and *Hab-1* sequences confirmed that KR binds to the consensus sequence and that binding is disrupted by the *Hab-1* lesion (Fig. 3). Although we cannot formally exclude the possibility that some other protein also binds to this site, we were able to confirm the importance of

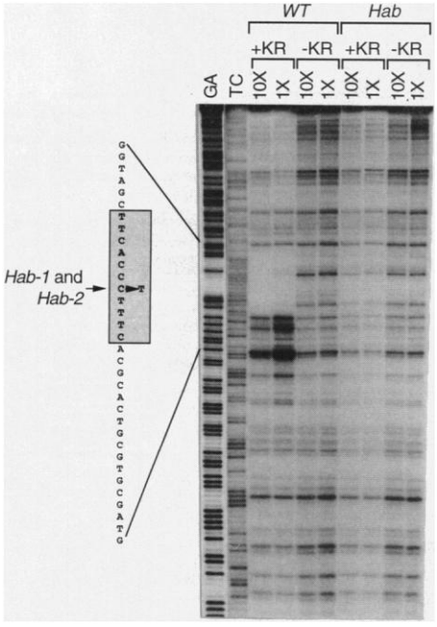

Fig. 3. The DNase I footprinting of KR protein to *WT* and *Hab-1* mutant sequences. Lanes labeled *WT* illustrate the DNase I cleavage ladder of a 147-bp HinP I fragment (coordinates 171 to 318, Fig. 2B) from the *iab-2(1.7)* fragment. Lanes labeled *Hab* show the DNase I cleavage ladder of an identically engineered piece of DNA from the *Hab-1* mutant. In lanes labeled +KR or −KR, protein extracts (1X = 8 μg, 10X = 80 μg) were used from KR expressing (+) or nonexpressing (−) bacterial cells (*39*). Maxam-Gilbert sequencing reactions are shown in the leftmost lanes (GA and TC). The sequences shown is the opposite from that shown in Fig. 2B.

Krüppel protein concentration in the generation of the *Hab* phenotype, by asking whether the penetrance of the *Hab* phenotype was affected in a *Kr* heterozygote. We found that in a *Kr/+;Hab-1/+* background, the number of flies exhibiting a *Hab* phenotype increases to 19% (268 flies scored), compared to the 1.5% (785 flies scored) exhibited by sibling flies carrying the CyO balancer chromosome (*+/CyO;Hab-1/+*). Animals of the genotype *Kr/+* also show a weakly penetrant gain-of-function phenotype that partially overlaps the *Hab* phenotype. In control crosses, we found that the penetrance of the *Kr*-dominant phenotype was only 3.5% (254 flies scored). Taken together, these results demonstrate that KR, acting through the *iab-2* region, represses the expression of *abd-A* anterior to PS 7. This finding fulfills the prediction made by Lewis "that *Hab* damages a regulatory element adjacent to [*abd-A*] in such a way as to reduce its affinity for a repressor" (*4*).

The *Krüppel* gene has been implicated to play both active and repressive roles in early *Drosophila* development (*32*). The *Kr* gene product is a zinc finger protein that forms a bell-shaped concentration gradient within the central portion of the *Drosophila* embryo (*32, 33*). In pre-cellular embryos, the central domain of KR expression accumulates peak levels of protein in PS 6 and 7. Protein levels fall off sharply on either side of this domain, such that no protein is detected anterior of PS 3 or posterior of PS 9. The region-specific repression that we observe (in PS 3 to 5, but not in PS 7 to 9) may reflect either the interaction with a second anteriorly localized protein such as *hunchback* or a difference in the way that KR binds at high and low concentrations (or both). Recent experiments have demonstrated that at high concentrations KR can bind to a single site as a dimer, whereas at low concentrations it occupies the same site as a monomer (*34*). This alteration in binding stoichiometry could influence in vivo protein-protein interactions. We note that several HB binding sites exist within the *iab-2(1.7)* initiator (Fig. 2B), and we speculate that efficient repression anterior to PS 7 could require the binding of both HB and KR proteins and perhaps a physical interaction between the two.

The pair-rule nature of the *iab-2(1.7)/LacZ* expression suggests that stripe formation also involves a pair-rule gene product. A likely candidate is the *even-skipped* protein, which both binds to the *iab-2(1.7)* fragment and is required for *iab-2(1.7)* activity (*31*). These observations suggest that the *iab-2(1.7)* initiator is similar to that of other previously described bithorax enhancers from the *bx* and *pbx* regions that appear to set early spatial expression domains through short-range interactions between pair-rule activators and gap-gene repressors (*9–11*). Because none of these isolated elements faithfully reproduce a complete homeotic expression pattern, however, it has been difficult to assess their roles within the intact bithorax complex. The results described here demonstrate that individual regulatory elements do contribute to the control of homeotic genes within intact complexes.

Point mutations in the regulatory sequences of higher eukaryotes are very rare. One of the few cases in which regulatory point mutations cause a phenotype is in the β-globin cluster, where lesions in the CCAAT and TATA boxes have been associated with certain forms of β thalassemia (*35*). In another case, a single base change that prevents the binding of the GATA1 transcription factor causes the Greek form of hereditary persistence of fetal hemoglobin (*36*). In *Drosophila*, a single base-sequence polymorphism within the *rosy* promoter has been shown to alter levels of *rosy* gene expression (*37*). The rarity of regulatory point mutations probably reflects both a small target size and several forms of regulatory redundancy. It is also possible that many regulatory mutations cannot be recovered because they produce severe phenotypic consequences, such as dominant lethal mutations.

The recovery of two independent mutations at the same base within the *iab-2* regulatory sequences is unusual. The homeotic transformation obviously contributed to the isolation of these mutants, but it is curious that, with perhaps hundreds of regulatory-protein binding sites within homeotic gene clusters, more mutations of this type have not been isolated. The explanation may lie in an unusual combination of circumstances that is peculiar to the structure of the *iab-2* initiator element. In many cases, individual control elements contain a multitude of binding sites for a given regulatory protein, and mutation in any one site may have only limited effects [for example, (*38*)]. In addition, control elements themselves may be redundant. Our analysis of the *iab-2* regulatory domain has revealed no other fragments capable of producing a pattern like that of *iab-2(1.7)*. This lack of control-element duplication, together with the single KR binding site may have made the *iab-2* initiation element especially susceptible to regulatory point mutations.

REFERENCES AND NOTES

1. M. Peifer, F. Karch, W. Bender, *Genes Dev.* 1, 891 (1987).
2. I. Duncan, *Annu. Rev. Genet.* 21, 285 (1987).

3. T. Kaufman, M. Seeger, G. Olsen, *Adv. Genet.* **27**, 309 (1990).
4. E. Lewis, *Nature* **276**, 565 (1978).
5. R. White and M. Akam, *ibid.* **318**, 567 (1985).
6. F. Karch, W. Bender, B. Weiffenbach, *Genes Dev.* **4**, 1573 (1990).
7. S. Celniker, D. Keelan, E. Lewis,, *ibid.* **3**, 1424 (1989).
8. R. Mann and D. Hogness, *Cell* **60**, 597 (1990).
9. S. Qian, M. Capovilla, V. Pirotta, *EMBO J.* **10**, 1415 (1991).
10. ———, *ibid.*, **12**, 3865 (1993).
11. C. Zhang, J. Müller, M. Hoch, H. Jäckle, M. Bienz, *Development* **113**, 1171 (1991).
12. R. White and R. Lehmann, *Cell* **47**, 311 (1986).
13. K. Harding and M. Levine, *EMBO J.* **7**, 205 (1988).
14. V. Irish, A. Martinez-Arias, M. Akam, *ibid.* **8**, 1527 (1989).
15. D. Lindsley and G. Zimm, Eds., *The Genome of* Drosophila melanogaster (Academic Press, San Diego, CA, 1992).
16. J. Reinitz and M. Levine, *Dev. Biol.* **140**, 57 (1990).
17. I. Duncan, personal communication; J. Simon, unpublished results.
18. The paradoxical transformation of haltere to wing may be caused by a low level of ABD-A protein that represses *Ubx* but is not high enough to transform cells to A2. As a result, a *Ubx* loss-of-function transformation is observed.
19. L. Frischer, F. Hagen, R. Garber, *Cell* **47**, 1017 (1986).
20. E. Jorgenson and R. Garber, *Genes Dev.* **1**, 544 (1987).
21. S. Celniker and E. Lewis, *Proc. Natl. Acad. Sci. U.S.A.* **90**, 1566 (1993).
22. H. Gyurkovics, J. Gausz, J. Kummer, F. Karch, *EMBO J.* **9**, 2579 (1990).
23. D. Cribbs, A. Pattatucci, M. Pultz, T. Kaufman, *Genetics* **132**, 699 (1992).
24. F. Karch, W. Weiffenback, J. Simon, W. Bender, unpublished data.
25. J. Simon, M. Peifer, W. Bender, M. O'Connor, *EMBO J.* **9**, 3945 (1990).
26. J. Simon, A. Chiang, W. Bender, M. J. Shimell, M. O'Connor, *Dev. Biol.* **158**, 134 (1993).
27. An EMBL3 library was constructed from *Hab-1* homozygotes, and the *Hab-1* containing phage was identified by hybridization with the 11.0-kb Sal I fragment illustrated in Fig. 2A. The *Hab-1* and Canton S 1.7-kb Sal I–Xba I subfragments from the 11.0-kb Sal fragment were cloned into the *Ubx/LacZ* reporter vector described by Qian, Capovilla, and Pirrota (*9*) and integrated into the *Drosophila* genome by P element–mediated germline transformation [G. M. Rubin and A. C. Spradling, *Science* **218**, 348 (1982)]. The w^+ transformant lines were established and examined for *LacZ* expression by in situ hybridization [D. Tautz and C. Pfeifle, *Chromosoma* **98**, 81 (1989)] or by staining with anti–β-galactosidase antibody (*25*). Antisense *LacZ* RNA was prepared from a pBluescript II KS(+) vector (Stratagene) containing the *LacZ*-coding region. The plasmid was linearized with Eco RI, and the digoxygenin-labeled *LacZ* probe was prepared by T7 transcription in the presence of digoxigenin uridine triphosphate. Hybridizations, washes, and histochemical staining were performed according to the procedures of J. Jiang, D. Kosman, T. Ip, and M. Levine [*Genes Dev.* **5**, 1881 (1991)]. Embryos were mounted in a solution of 70% glycerol for photography.
28. The 1.7-kb Sal I–Xba I fragment shown in Fig. 2A was subcloned in Bluescript II KS+ (Stratagene) and sequenced with standard methods. The background chromosome from bx^6/*Df(P2)* flies was also cloned and sequenced. The bx^6 allele was obtained in the same mutagenic screen as *Hab-1* and should be isogenic to *Hab-1* at all bases except for that which represents the *Hab-1* lesion (E. B. Lewis, personal communication). Chromosomal DNA from *Hab-2/Df(P2)* flies was amplified by PCR with the use of the 1-2 and 3-4 pairs of primers indicated in Fig. 2B. To eliminate PCR artifacts, the amplified products were sequenced directly with the use of the Silver sequence system (Promega, Madison, WI). The background chromosome for *Hab-2* was Canton S, and its entire 1.7-Kb Sal I–Xho I fragment was sequenced by standard methods.
29. To examine the effects of gap and pair-rule gene products on the expression of the *iab-2(1.7)* fragment, transformant lines containing this construct where crossed into the following mutant backgrounds: hb^{14F}, Kr^2, kni^{ID}, gt^{YA}, tll^{110} eve^{R13}, and *Df(2R) Scb (ftz)*. All mutants except *ftz* altered the pattern, but only *Kr* mutants showed an expression pattern reminiscent of that produced by the *Hab* mutants.
30. J. Treisman and C. Desplan, *Nature* **341**, 335 (1989).
31. M. Shimell and M. O'Connor, unpublished data.
32. M. Pankratz and H. Jäckle, in *The Development of* Drosophila melanogaster, M. Bate and A. Martinez-Arias, Eds. (Cold Spring Harbor Laboratory Press, Cold Spring Harbor, NY, 1993), pp. 467–517.
33. U. Rosenberg *et al.*, *Nature* **319**, 336 (1986).
34. F. Sauer and H. Jäckle, *ibid.* **364**, 454 (1993).
35. H. Kazazian *et al.*, *Cold Spring Harbor Symp. Quant. Biol.* **51**, 371 (1986).
36. M. Berry, F. Grosveld, N. Dillon, *Nature* **358**, 499 (1992).
37. D. Curtis, S. Clark, A. Chovnick, W. Bender, *Genetics* **122**, 653 (1989).
38. W. Driever, G. Thomas, C. Nüsslein-Volhard, *Nature* **340**, 363 (1992).
39. KR protein was produced in BL21 (DE3) cells containing plasmid pARKr [D. Stanojevic, T. Hoey, M. Levine, *ibid.* **341**, 331 (1989)]. Protein extracts were prepared from cells containing or lacking the pARKr plasmid [F. Studier, A. Rosenberg, J. Dunn, J. Dubendorff, *Methods Enzymol.* **185**, 60 (1990), as modified by T. Hoey and M. Levine, *Nature* **332**, 858 (1988)]. Protein determinations were made with the Pierce BCA protein assay kit. For footprinting experiments, DNA fragments were end-labeled with ^{32}P by a Klenow fill-in reaction. The footprinting procedure was carried out as described by Stanojevic *et al.* (above). with the following changes: The 50-ml binding reaction was composed of 100 mM KCl, 35 mM Hepes (pH 7.9), 10 mM $MgCl_2$, 1 mM dithiothreitol, 0.1 mM $ZnCl_2$, 12% glycerol, and 0.06% Nonidet P-40 and included 50,000 counts of end-labeled DNA, 2 μg of poly (dI-dC) (Pharmacia), and 5 μl of protein extract in 4 M urea and Z buffer (T. Hoey and M. Levine, above). Either 24 or 48 ng of DNase I was used in the footprinting reactions, which proceeded for 4 min on ice and were stopped by the addition of EDTA (to 50 mM) and phenol. The reactions were electrophoresed in 6% polyacrylamide–8 M urea wedge gels. The sequencing reactions were a modified version of A. Maxam and W. Gilbert [D. Bencini, G. O'Donovan, J. Wild, *BioTechniques* **2**, 4 (1984)].

40. We thank E. Lewis and I. Duncan for sharing mutant stocks and for many informative discussions on the origin and properties of *Hab* mutations; special thanks is also due to I. Duncan for suggesting that we look at the penetrance of the *Hab* phenotype in a *Kr* heterozygote. We also thank J. Treisman and C. Desplan for the antisense *LacZ* plasmid; C. Desplan for the pARKr plasmid; T. D. Nguyen for making a nested deletion series for the sequencing of the Canton S *iab-2(1.7)* fragment; and L. Marsh and R. Warrior for comments on the manuscript. Supported by grants from PHS (M.B.O. and W.B.), a fellowship from the Medical Foundation/Charles King Trust (J.S.), and a University of Minnesota McKnight Land grant (J.S.).

13 December 1993; accepted 29 March 1994

Cloning of a Grb2 Isoform with Apoptotic Properties

Isabelle Fath, Fabien Schweighoffer, Isabelle Rey, Marie-Christine Multon, Janine Boiziau, Marc Duchesne, Bruno Tocqué*

Growth factor receptor–bound protein 2 (Grb2) links tyrosine-phosphorylated proteins to a guanine nucleotide releasing factor of the son of sevenless (Sos) class by attaching to the former by its Src homology 2 (SH2) moiety and to the latter by its SH3 domains. An isoform of *grb2* complementary DNA (cDNA) was cloned that has a deletion in the SH2 domain. The protein encoded by this cDNA, Grb3-3, did not bind to phosphorylated epidermal growth factor receptor (EGFR) but retained functional SH3 domains and inhibited EGF-induced transactivation of a Ras-responsive element. The messenger RNA encoding Grb3-3 was expressed in high amounts in the thymus of rats at an age when massive negative selection of thymocytes occurs. Microinjection of Grb3-3 into Swiss 3T3 fibroblasts induced apoptosis. These findings indicate that Grb3-3, by acting as a dominant negative protein over Grb2 and by suppressing proliferative signals, may trigger active programmed cell death.

We screened 500,000 recombinant phages carrying DNA from human placenta with an oligonucleotide probe derived from the human *grb2* sequence (*1*). Nine of ten clones contained inserts that were identical to the *grb2* sequence; however, we identified one clone with a deletion in the SH2 domain (*2*). Analysis of the remaining sequence revealed an identity with *grb2*, even in the 5′ and 3′ noncoding regions. The open reading frame of the cloned DNA encoded a 177–amino acid sequence with two SH3 domains flanking the incomplete SH2 domain (Fig. 1). The amino acids deleted in the SH2 domain (amino acids 60

Rhône-Poulenc Rorer, Centre de Recherche de Vitry-Alfortville, 13 quai Jules Guesde-BP14, 94403 Vitry sur Seine Cedex, France.

*To whom correspondence should be addressed.